Analysis of polarization states in magneto-optic fiber Bragg gratings based on a nonmagnetic equivalent model

Baojian Wu
Xiaojing Zhou
Kun Qiu
University of Electronic Science and Technology of China
Key Lab of Broadband Optical Fiber Transmission and Communication Networks of the Ministry of Education
Chengdu 610054, China
E-mail: bjwu@uestc.edu.cn

Abstract. According to the magneto-optic coupling characteristics of magneto-optic fiber Bragg gratings (MFBGs), we present a nonmagnetic equivalent model of a uniformly magnetized MFBG to analyze the optical polarization states output from the MFBG for incident linearly polarized light. The Faraday rotation of transmitted light is enhanced at the edges of a grating bandgap, and then can be applied to the measurement of a magnetic field by employing the wavelength speeding method. The use of apodized MFBGs helps to simultaneously achieve a good linear magnetic field response and extremely small fluctuation of transmittivity. For a typical paramagnetic terbium-doped and apodized MFBG, the temperature coefficient of the Faraday rotation is calculated to be -2.5×10^{-4} m/K.
[DOI: 10.1117/1.3484951]

Subject terms: magneto-optic fiber Bragg grating; Faraday effect; polarization; magnetic field sensor; software simulation.

Paper 100242R received Mar. 25, 2010; revised manuscript received Jul. 1, 2010; accepted for publication Jul. 12, 2010; published online Sep. 2, 2010.

1 Introduction

Magneto-optic fiber Bragg gratings (MFBGs) are a class of special fiber Bragg gratings (FBGs) associated with magneto-optical (MO) effects, and can be regarded as 1-D photonic crystals with magnetically tunable photonic bandgaps (PBGs).[1,2] Conventional FBGs used in optical communications and fiber sensing can be regarded as MFBGs to a certain extent if the weak MO effects in the fibers are taken into account. However, to utilize the intrinsic MO effects in silica FBGs, one has to recur to some high-resolution detection technologies such as unbalanced Mach-Zehnder interferometers[3] and polarization-dependent loss (PDL).[4] On the other hand, some rare-earth-doped FBGs with large MO coefficients are expected to become the desirable MFBGs. For example, the 65-wt% terbium-doped silicate fiber possesses an effective Verdet constant of −32.1 rad/(T.m), which is 27 times larger than that of silica fibers.[5] For the photosensitization of terbium-doped alumino-silicate fibers, refractive index modulations as high as 6×10^{-4} through high pressure H_2 loading can be achieved.[6] The promising MFBGs have some potential applications in novel current or magnetic field sensors,[7] nonlinear MO switches,[8] and tunable dispersion compensation modules.[9]

For the uniform MFBG, the analytic expression for transmittivity or reflectivity has been deduced from the MO coupled-mode theory[2] and then is used to explain magnetic field dependency of polarization-dependent loss (PDL) in the experiments.[4] In contrast, it is difficult to obtain the analytical solution of optical field in nonuniform MFBGs. In this case, one has to adopt the transfer matrix method to numerically deal with the nonuniform MFBGs by using the piecewise-uniform MFBG model.[9] In this work, we take advantage of some commercially avaliable simulation softwares, such as the Optisystem (OptiWave, Ottawa, Ontario, Canada), to conveniently simulate the nonuniform MFBGs by means of their nonmagnetic equivalent model, in which a nonuniform MFBG at homogeneous magnetization is equivalent to the nonmagnetic FBG with a modified effective refractive index dependent on the applied magnetic field. Instead, the refractive index modulation of the nonmagnetic equivalent FBG stays the same as the nonuniform MFBG. As an example, the nonmagnetic equivalent model is used to analyze the magnetic field dependency of polarization states of transmitted and reflected light output from the MFBGs. The enhancement of the Faraday rotation and ellipticity angles in the vicinity of the photonic bandgap (PBG) edges is investigated in detail. The measurement of magnetic field can be implemented effectively by sweeping the peak value of the transmitted Faraday rotation, just like the measurement of peak PDL. In addition, the optimization of the MFBG's apodization function helps to improve the linear response of magnetic field and reduce the fluctuation of output power. Finally, we make a computation with the temperature coefficient of the Faraday rotation in the terbium-doped and apodized MFBG.

2 Nonmagnetic Equivalent Model of the Magneto-Optic Fiber Bragg Gratings

Generally speaking, the unhomogeneity of a so-called nonuniform MFBG can be attributed to the change of refractive index modulation or/and magnetization[9,10] within the fiber core. In this work, we only take into account the former, namely, uniformly magnetized MFBG, also called nonuniform MFBG, for convenience.

0091-3286/2010/$25.00 © 2010 SPIE

In a single-mode MO fiber with neglectable linear birefringence, there always exist two orthogonal eigenmodes, left- and right-handed circularly polarized (LCP and RCP) light. When an isotropic perturbation of refractive grating independent of the eigenmodes is added to the MO fiber, the identically polarized guided waves propagating forward and backward are coupled with each other. According to the coupled-mode analysis used in Ref. 2, grating perturbation does not change the polarization state of the eigenmodes, but has a great influence on the amplitude distribution of the optical field. For the nonuniform MFBG, one can always divide the whole MFBG into many uniform grating segments, similar to the piecewise-uniform FBG model,[11] and in each segment the grating period and magnetization are fixed. Thus, the steady-state propagation characteristics of the eigen LCP and RCP light in the whole MFBG can be well known by orderly multiplying the transfer matrices of the uniform grating segments.

For a nonuniform MFBG, let us consider any given uniform segment from $z=z_{n-1}$ to $z=z_n=z_{n-1}+h$, in which the grating perturbation is taken in the form of $\Delta n(z)=2\Delta n_g \cos(2\pi z/\Lambda)$, where $2\Delta n_g$ and Λ are respectively the ac index modulation and the local grating period. In this case, the complex amplitudes of the guided light $A_p^{\pm}(z,t)$ can be given as follows:[9]

$$\begin{bmatrix} A_p^+(z_n) \\ A_p^-(z_n) \end{bmatrix} = T_{n,n-1}(\delta_p,h) \begin{bmatrix} A_p^+(z_{n-1}) \\ A_p^-(z_{n-1}) \end{bmatrix}, \tag{1}$$

where the subscript p represents the LCP or RCP eigenmode, the superscript "±" corresponds to the forward and backward propagation respectively, and the transfer matrix is expressed as

$$T_{n,n-1}(\delta_p,h) = \frac{1}{q_p} \begin{bmatrix} q_p \cos(q_p h) + i\delta_p \sin(q_p h) & i\kappa_g \sin(q_p h) \\ -i\kappa_g \sin(q_p h) & q_p \cos(q_p h) - i\delta_p \sin(q_p h) \end{bmatrix}, \tag{2}$$

in which $q_p=(\delta_p^2-\kappa_g^2)^{1/2}$, $\delta_p=\beta_p(\omega)-\beta_B$, $\beta_p=\bar{n}_p k_0$, and $\beta_B=\pi/\Lambda$; $\bar{n}_p=n_0 \pm \kappa_m/k_0$ are the effective refractive indices of the MFBG for the RCP and LCP eigenmodes, and n_0 is the intrinsic average refractive index of the nonuniform MFBG; $\kappa_g=k_0\Delta n_g$ is the grating coupling coefficient, $\kappa_m=V_B B$ is the MO coupling coefficient associated with the Verdet constant V_B and magnetic induction B; and k_0 is the lightwave number in vacuum. From Eq. (2), each uniform MFBG segment can be equivalent to the nonmagnetic uniform FBG, whose modal index is equal to the effective refractive index $\bar{n}_p=n_0 \pm \kappa_m/k_0$, and then the whole nonuniform MFBG at homogeneous magnetization has the same modal index, independent of the refractive index distribution of the MFBG. Thus, the nonmagnetic equivalent model of the MFBG is also described as follows: a uniformly magnetized MFBG can be equivalent to the nonmagnetic FBG with the magnetic-field-dependent modal index $\bar{n}_p$, and the refractive index modulation of the equivalent FBG is identical to that of the MFBG. Note that the effective refractive index $\bar{n}_p$ only applies to the eigenmodes, and an isotropic grating perturbation has no influence on the eigen states of polarization (SOPs) in the MO fiber.

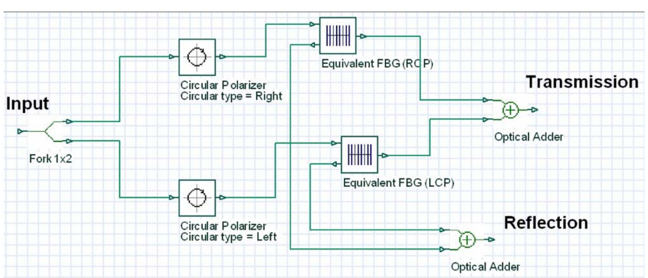

Fig. 1 The equivalent model of the MFBG in the Optisystem simulation.

According to the MFBG's nonmagnetic equivalent model, the Optisystem simulation system of the MFBG is established, as shown in Fig. 1. The circular polarizers are used to extract the RCP and LCP components from the incident light, which is regarded as the superposition of the two orthogonal eigenmodes. Then, the RCP and LCP components are, respectively, input to individual nonmagnetic equivalent FBG. Finally, the optical adders combine the two transmitted (or reflected) optical fields into the output of the nonuniform MFBG. In the Optisystem simulation, the equivalent FBGs need to be configured through some parameters, including: 1. modal index $n_{\mathrm{eff}}=\bar{n}_p$; 2. centeral wavelength $\lambda_B=2n_{\mathrm{eff}}\Lambda_0=\lambda_0[1 \pm \Lambda_0\kappa_m/\pi]$, in which Λ_0 and $\lambda_0=2n_0\Lambda_0$ are the grating period and the reference wavelength, respectively; and 3. the other parameters, such as the grating length L, and the ac and dc index modulations ($\Delta n_{\mathrm{AC}}=2\Delta n_g$ and Δn_{DC}), which take the same values as the MFBG. The validity of the nonmagnetic equivalent model of the MFBG can be made sure by comparing the simulation data output from the Optisystem optical filter analyzer with the theoretical results derived from the analytical expressions[2] and the piecewise-uniform method.[9]

3 Analysis of Polarization States in Unform and Apodized Magneto-Optic Fiber Bragg Gratings

In what follows, we make use of the nonmagnetic equivalent model of the MFBG to investigate the output SOP evolvement for the incident linearly polarized (LP) light. The transmitted and reflected SOPs in terms of the principal azimuth and ellipticity angles, ψ and χ, can be measured by using the polarization analyzer in the Optisystem

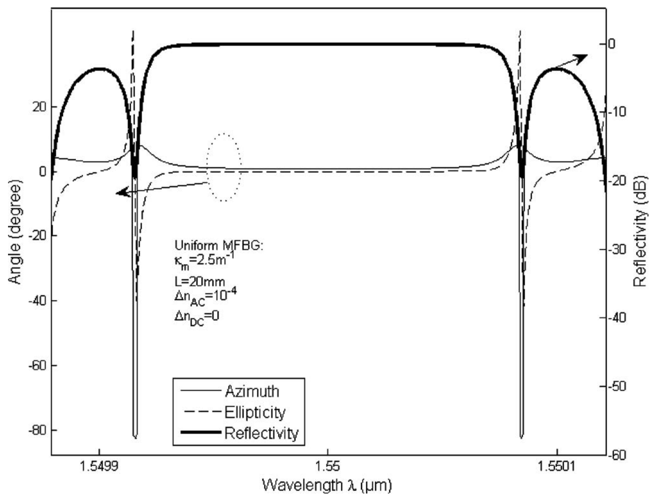

Fig. 2 The SOP characteristics of reflected light for the uniform MFBG.

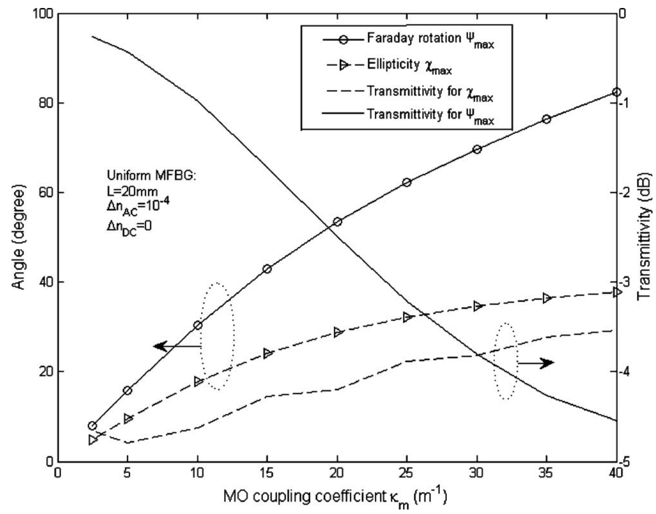

Fig. 4 Variations of maximal azimuth and ellipticity angles with the MO coupling coefficient for the uniform MFBG.

software. The frequency dependence of the transmitted azimuth angle is also called the Faraday rotation spectrum if the azimuth angle of incident LP light is taken as $\psi=0$. In our simulation, the common grating parameters are used as follows: $n_0=1.45$, $\Lambda_0=534.5$ nm, $\lambda_0=1550$ nm, $L=20$ mm, $\Delta n_{\mathrm{AC}}=10^{-4}$, and $\Delta n_{\mathrm{DC}}=0$.

First, we take an example for the uniform MFBG with $\kappa_m=2.5\ \mathrm{m}^{-1} \ll \kappa_g$, corresponding to $B=0.125$ T for the terbium-doped optical fiber with the Verdet constant $V_B=20\ \mathrm{rad}/(\mathrm{T}\cdot\mathrm{m})$,[12] and the polarization characteristics of reflected and transmitted light are respectively plotted in Figs. 2 and 3. Obviously, they have a different polarization transformation. From Fig. 2, it is difficult to measure the maximal azimuth or ellipticity angle of the reflected light, since the corresponding wavelength falls very close to the minima in the reflection spectra. In contrast, for the transmitted light, the maximal azimuth and ellipticity angles occur at the wavelength of large transmittivity, as shown in Fig. 3. Thus, the magnetic field response of the MFBG can be investigated by means of the maximal azimuth or ellipticity for the transmitted light, instead of the reflected light.

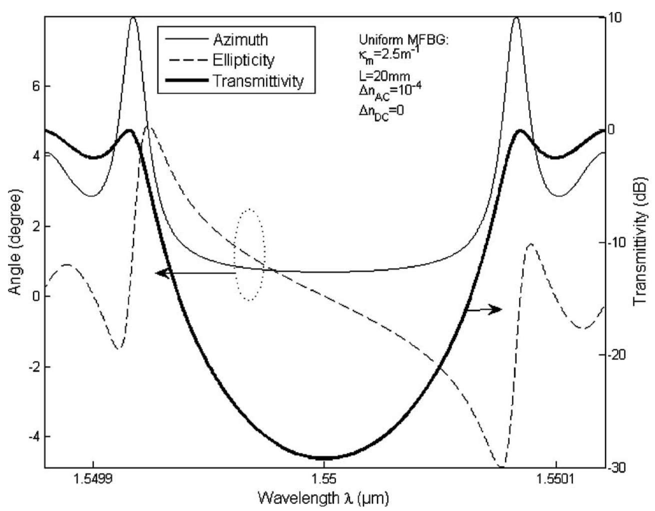

Fig. 3 The SOP characteristics of transmitted light for the uniform MFBG.

Next, we discuss the influence of the MO Faraday effect on the transmitted SOPs and the magnetic field response of the MFBG. From Fig. 3, the Faraday rotation $\psi(\lambda)$ is expressed as $\psi(\lambda)=\alpha(\lambda)\kappa_m L$, where $\alpha(\lambda)$ is called the Faraday enhancement factor. it is seen that: 1. at the wavelength far away from the photonic bandgap (PBG) λ_∞, the Faraday rotation is just as it is in the MO fiber and $\alpha(\lambda_\infty)=1$; 2. at the central wavelength, the Faraday enhancement factor takes a minimal value ($\alpha_{\min}=0.247$) and the Faraday rotation is reduced; and 3. the maximum Faraday rotation $\psi_{\max}$ with $\alpha_{\max}=2.77$ exists in the vicinity of the PBG edge, which can be explained from the multiple reflection of light and the nonreciprocity of Faraday effect.[11] By the way, the maximum ellipticity angle $\chi_{\max}$ and the Faraday rotation $\psi_{\max}$ occur at the same PBG edge, but the corresponding wavelengths have a small difference.

In practice, just as with the peak PDL measurement, the maximal values of $\psi_{\max}$ and $\chi_{\max}$ may as well be measured by the wavelength sweeping method, regardless of the spectral width of angle enhancement and the accurate control of wavelength to a certain extent. Figure 4 shows the variations of the maximal azimuth and ellipticity angles $\psi_{\max}$ and $\chi_{\max}$ with the MO coupling coefficient κ_m for the uniform MFBG. The corresponding transmittivity is also plotted in Fig. 4. It is clear that with the increase of κ_m, $\psi_{\max}$ or $\chi_{\max}$ is improved, but the transmittivity is accordingly reduced in the range of less than 3 dB for $\kappa_m \leqslant 20\ \mathrm{m}^{-1}$.

Of course, the previously mentioned procedure can also be applied to the nonuniform MFBG at homogeneous magnetization. For the Gaussian apodized grating structure, Faraday enhancement reduces slightly compared with the case for the uniform MFBG, as illustrated in Fig. 5. However, the apodized MFBG possesses two unique advantages: linear magnetic field response and small power fluctuation. In this case, one may prefer the $\psi_{\max}$-based measurement of magnetic field, since the azimuth sensitivity $\psi_\kappa=d\psi_{\max}/d\kappa_m \approx 1.475\ \mathrm{deg}/(\mathrm{rad}\cdot\mathrm{m}^{-1})$ is about three

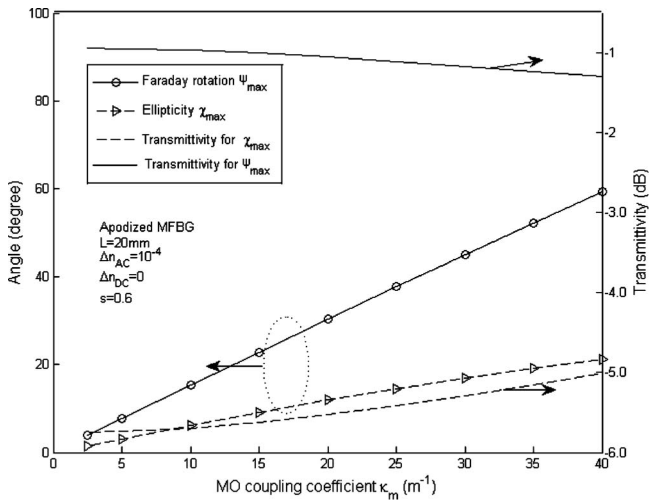

Fig. 5 Variations of maximal azimuth and ellipticity angles with the MO coupling coefficient for the Gaussian apodized MFBG with $s=0.6$.

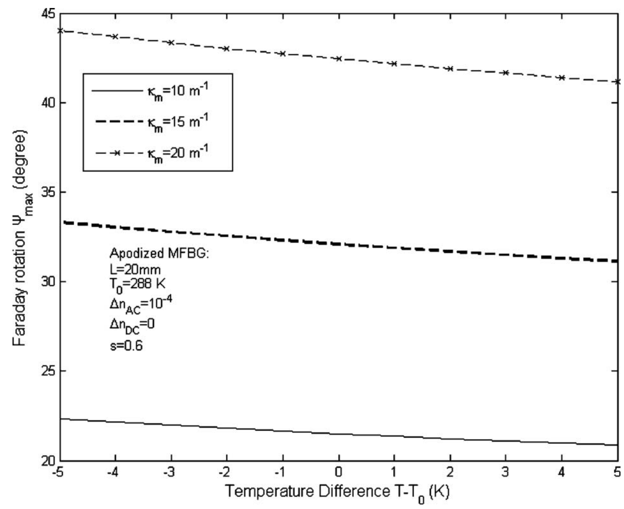

Fig. 6 Temperature dependence of the Faraday rotation for the apodized MFBG.

times more than that of $\chi_{\max}$. In addition, the apodization function of the nonuniform MFBG should be optimized for the tradeoff between the linear response and the rotation enhancement, according to the dynamic range of applied magnetic field.

Finally, we discuss the fluctuation of the Faraday rotation caused by temperature change for the apodized MFBG. The temperature change in the environment will mainly lead to variations of the refractive index $n_0(T)$, the grating period $\Lambda_0(T)$, and the MO coupling coefficient $\kappa_m(T)$, which are respectively related to the thermo-optic effect, the thermal expansion, and the temperature dependence of the Verdet constant. For a small temperature change, the physical parameters mentioned before can be expressed in the forms:

$$n_0(T) = n_0(T_0)[1 + \alpha_n(T - T_0)], \tag{3}$$

$$\Lambda_0(T) = \Lambda_0(T_0)[1 + \alpha_\Lambda(T - T_0)], \tag{4}$$

$$\kappa_m(T) = \kappa_m(T_0)[1 + \alpha_V/(T - T_P)], \tag{5}$$

where α_i $(i=n,\Lambda,\kappa)$ are the relevant coefficients and Eq. (5) is satisfied for the paramagnetic terbium-doped fiber.[13] As a result, the MFBG's effective refractive index and Bragg wavelength can be written as follows:

$$n_{\text{eff}}(T) = n_0(T)[1 \pm \Lambda_0(T)\kappa_m(T)/\pi], \tag{6}$$

$$\lambda_B(T) = \lambda_0(T)[1 \pm \Lambda_0(T)\kappa_m(T)/\pi], \tag{7}$$

where $\lambda_0(T)=2n_0(T)\Lambda_0(T)$. Figure 6 plots the temperature dependence of the Faraday rotation for the apodized MFBG under the different magnetic fields of $B=0.5$ T, 0.75 T, and 1 T, respectively corresponding to $\kappa_m(T_0)=10$, 15, and 20 m^{-1} with the Verdet constant $V_B=20$ rad/(T·m). The following parameters are used in our calculation: $T_0=288$ K, $\alpha_n=6\times10^{-6}$ K^{-1}, $\alpha_\Lambda=4.4\times10^{-6}$ K^{-1},[12] $\alpha_V=17.6$ K, and $T_P=245.4$ K.[13] From Fig. 6, the Faraday rotation $\psi_{\max}$ is almost inversely proportional to temperature T in a small range of temperature change. The temperature coefficient of the Faraday rotation can as well be derived from Fig. 5 and Eq. (5) as follows:

$$\alpha_F = \frac{d\psi_{\max}}{\kappa_m dT} = \frac{d\kappa_m}{\kappa_m dT}\frac{d\psi_{\max}}{d\kappa_m} = -\frac{\alpha_V\psi_\kappa}{(T-T_P)^2} \approx -0.0143\ \text{deg}/(\text{rad}\cdot\text{m}^{-1}\ \text{K}) \quad \text{at} \quad T=288\ \text{K} = -2.496\times10^{-4}\ \text{m/K}, \tag{8}$$

which is identical with the results illustrated in Fig. 6. It is clear that the temperature coefficient of the Faraday rotation α_F is dependent on the temperature characteristic of the Verdet constant and the magnetic field sensitivity of the Faraday rotation.

4 Conclusion

To take advantage of commercially available simulation software to analyze the transmission characteristics of the nonuniform MFBG, we have proposed the nonmagnetic equivalent model of the MFBG, that is, a uniformly magnetized MFBG is equivalent to the nonmagnetic FBGs, in which the modal index is equal to the effective refractive index $\bar{n}_p=n_0\pm\kappa_m/k_0$, and the corresponding central wavelength needs to be modified as well. The validity of the MFBG's nonmagnetic equivalent model is made sure by using the Optisystem optical filter analyzer. The polarization properties of the transmitted and reflected light, in terms of the azimuth and ellipticity angles, are in detail investigated for the uniform and apodized MFBGs by the Optisystem simulation. It is shown that the enhanced Faraday rotation of the transmitted light can be used to measure the response of the MFBG to the applied magnetic field by sweeping the peak value of the Faraday rotation. The apodized MFBG has better linear dynamics than the uniform MFBG. For the paramagnetic terbium-doped apodized MFBG, the temperature dependence of the Faraday rotation is analyzed, and the temperature coefficient is determined by the Verdet constant and magnetic field sensitivity. The combination of the nonmagnetic equivalent model and the existing simulation software helps to develop the MFBG-based optical signal processing devices with application to optical fiber communications and the sensing area.

Acknowledgment

This work was supported by the National High Technology Research and Development Program of China (863 Program) number 2009AA01Z216, and by the Program for New Century Excellent Talents in University (NCET).

References

1. J. L. Arce-Diego, R. López-Ruisánchez, J. M. López-Higuera, and M. A. Muriel, "Fiber Bragg grating as an optical filter tuned by a magnetic field," *Opt. Lett.* **22**, 603–605 (1997).
2. B. J. Wu, X. Liu, and K. Qiu, "Characteristics of magneto-optic fiber Bragg gratings for use in optical signal processing," *Opt. Fiber Technol.* **15**, 165–171 (2009).
3. A. D. Kersey and M. J. Marrone, "Fiber Bragg grating high-magnetic-field probe," *Proc. SPIE* **2360**, 53–56 (1994).
4. H. Peng, Y. Su, and Y. Q. Li, "Analysis of a new measurement for electromagnetic with fiber grating," *Proc. SPIE* **7134**, 71342C (2008).
5. L. Sun, S. Jiang, and J. R. Marciante, "Compact all-fiber optical Faraday isolator," *Proc. SPIE* **7580**, 0277–786X (2010).
6. T. Taunay, P. Bernage, G. Martinelli, et al., "Photosensitization of terbium doped alumino-silicate fibres through high pressure H_2 loading," *Opt. Commun.* **133**, 454–462 (1997).
7. B. J. Wu, Y. Yang, and K. Qiu, "Magneto-optic fiber Bragg gratings with application to high-resolution magnetic field sensors," *J. Electron. Sci. Technol. China* **6**, 423–425 (2008).
8. K. Qiu, B. J. Wu, and F. Wen, "Nonlinear propagation of circularly polarized light in magneto-optic fiber Bragg gratings," *Acta Phys. Sin-Ch. Ed.* **58**, 1726–1730 (2009).
9. B. J. Wu, X. Lu, and K. Qiu, "Magneto-optic fiber gratings useful for dynamic dispersion management and tunable comb filtering," *Chin. Phys. Lett.* **27**, 067803-1-4 (2010).
10. K. S. Lee, "Polarization mode coupling in circularly birefringent gratings," *Appl. Opt.* **43**, 4393–4398 (2004).
11. T. Erdogan, "Fiber grating spectra," *J. Lightwave Technol.* **15**, 1277–1294 (1997).
12. J. Ballato and E. Snitzer, "Fabrication of fibers with high rare-earth concentrations for Faraday isolator applications," *Appl. Opt.* **34**, 6848–6854 (1995).
13. N. Di, J. Zhao, Y. Jiang, et al., "Experiment research on temperature response of Faraday effect in paramagnetic Terbium glass," *Acta Photonica Sin.* **35**, 1645–1648 (2006).

Baojian Wu graduated from Shanghai Jiaotong University, China. Now he is a professor and doctoral supervisor. His research interests include optical devices, optical fiber communications, optical information processing, etc. He is the author of more than 70 journal publications and the book *Theory of Microwave Magneto-Optics and Magneto-Optical Signal Processing* (UESTC Press, 2009). In the past five years, he has presided over four projects, including two projects of the National Natural Science Foundation of China (NSFC), one of the National High Technology Research and Development Program of China (863 Program), and one for the Program for New Century Excellent Talents in University (NCET). As a coinvestigator, he participated in the 863 Program and Sichuan Provincial basic application research projects. He was the recipient of the Second Prize of Provincial Sci-Tech Advancement Award by the Sichuan Provincial Government in 2007.

Xiaojing Zhou received her bachelor's degree in communication and information systems from Changchun University of Science and Technology in 2008. She is currently working toward the MS degree in the University of Electronic Science and Technology of China, where she is working on magneto-optic fibers and nonlinear effects and their applications in optical communications, fiber optical sensors, etc.

Kun Qiu received the MS (1987) and PhD (1990) degrees from Tsinghua University, and was Director of the State Key Laboratory of the Broadband Optical Transmission and Communication Network from 2002 to 2006. He is doing research on fiber optic communication theory and techniques. As a research team leader, he has finished more than 20 important projects. He is the owner of eight awards of science and technology progress from provinces or ministries. He is the author of more than 200 scientific papers and the book of *Introduction of Optical Communication* (UESTC Press, 2008).